CAFE

Calar Alto Fiber-fed Echelle spectrograph

www.caha.es/sanchez/cafe

Commissioning of the Instruments

First Results

Calar Alto Fiber-fed Echelle Spectrograph
CAFE Commissioning

Issue 1.1

29/07/2011

-

Authors	S.F.Sánchez & J. Aceituno
Contact	S.F.Sánchez (sanchez@caha.es)

This page was intentionally left blank

Change Record

Issue	Date	Section affected	Reason/Initiation/Documents/Remarks
1.0	01/07/2011	all	Creation by S.F.Sanchez .
1.01	10/07/2011	First Light	S.F.Sanchez .
1.02	20/07/2011	commissioning	S.F.Sanchez .
1.1	29/07/2011	CCD & Short Description	J.Aceitun .

This page was intentionally left blank

Contents

This page was intentionally left blank

1 Introduction

The Calar Alto Fiber-fed Echelle spectrograph is an instrument constructed at CAHA to replace FOCES, the high-resolution echelle spectrograph at the 2.2m Telescope of the observatory. FOCES is a property of the Munich University Observatory, and it has been removed from Calar Alto along 2010. The instrument comprises a sustantial fraction of the telescope time at observatory, and it is due to that it was taken the decission to build a replacement.

The basic characteristics of CAFE will be similar to those of FOCES. It will share the same spectral range and resolution, and the basic optical design. The main differences would be:

- CAFE will be installed in temperature and vibration control room, with a much sofisticated neumatic stabilization system install in the optical bench. This will guarantee a much better stability of the instrument, increasing its performance and accuracy for velocity measurements of fainter objects. The corresponding tests are still on progress, but the selected location seems to fulfill the considered requirements.

- The optical design of the camera of the instrument has been optimized, based on the knowledgement acquired with FOCES. We expect to increase the efficiency of the instrument in at least a 10% due this new optimized design CAFE will be equiped with a new CCD camera, and iKon-L, with 2048x2048 pixels of 13.5 mu. This camera has a better QE, lower readout-noise and higher read-out speed that the currently used in FOCES. We expect to increase the efficiency of the instrument by 15% by using this new CCD.

- In second phase, CAFE will be equiped with a Iodine-cell in order to perform self calibrations of the velocity measurements. This equipement will allow CAFE to perform observations with the accuracy required for the detection of exoplanets.

The instrument was integrated by the end of 2010, and has passed through its testing phase in the lab in the first months of 2011. It went to the telescope for its first light the 16th of May 2011, and it will be deliver to the community along this year.

1.0.1 The Consortium

CAFE is built by a Consortium leaded by CAHA, integrated by members of the Observatory of Munich University and the Astrophysics Departement of the University of Goettingen. Recently, the consortium has agregated new members from the CAB and the UCM. The current members of the collaboration are:

- Dr. Sebastian F. Sanchez (CAHA), PI of the project.

- Dr. Jesus Aceituno (CAHA), Project Manager and co-PI.

- Dr. Frank Grupp (USM), Design Advisor.

- Dr. Stefan Dreizler (UG).

- Dr. Jacob Bean (UG).

- Mr. Ulrich Thiele (CAHA).

- Dr. S.Pedraz (CAHA).

- Dr. L.Montoya (CAHA).

- Mr. D. Benitez (CAHA).

- Dr. M. Hernan Obispo (UCM), Science Advisor.

- Dr. D. Barrado (CAHA), Science Advisor.

CAFE has been build un behalf of the recommendations of the CAHA SAC, and EC. The total cost of the instrument, including both components and hand-work was below the foreseen 400k euros. Of them, 100k euros would be contributed by the University of Goettingen. The remaining money has been provided by the CAHA through requests of the PI to external Funding Agencies (Spanish Ministery of Science, ICTS-2008-24 & ICTS-2009-32, and Junta de Andalucía, P08-FWM-04319). The instrument has been built at basically zero cost for Calar Alto.

Table 1: Basic features of CAFE.

Design	Echelle spectrograph
Telescope	Calar Alto 2.2m
Resolution	62000 ± 5000
Wavelength	3960 - 9500A
Sensitivity	SNR $\sim$30 mag 14.5 and 2700sec
TELESCOPE MODULE	
Calibration lamps	Hal and ThAr
Aperture	2.4 arcseconds (200μm)
OPTICAL FIBER	
Type	Polymicro FBP100140170
Length	17.5m
Inner protection tube	ETFE with Kevlar for strain relief
Outer protection tube	stainless steel tube
Micro-lenses	N-F2, Both ends
SPECTROGRAPH	
Optical bench	2400 x 1200 x 203mm
Entrance slit width	100μm
Grating	31.6 g/mm BA[1]=63.9 degrees
Collimators[2]	OAP1 λ/20 FL=60.0" D=10.0" OAD=7.0"
	OAP2 λ/20 FL=60.0" D=10.0" OAD=9.0"
Prisms	LF5, Deviation angle 33ž
Camera	f/3
CCD	IKON-L DZ936 back illuminated
Pneumatic isolator	Newport I-2000

2 Short Description of the Instrument

The basic characteristics of CAFE are very similar to those of FOCES (Pfeiffer et al. 1998). It shares the same spectral range and resolution, and the basic concepts on optical design. Table 1 summarized the main features of the instrument. Despite that, some improvements have been included in the design to improve the current performance of FOCES. In particular, (i) a new optical design of the camera; (ii) a better efficiency of the transmission of the fiber. (ii) the optical quality of all the components has been selected to be $\lambda/20$, instead of the original $\lambda/=10$; (iii) an isolated room has been selected to place the instrument, thermalize and stabilized against vibrations; (iv) most of the mobile parts in FOCES has been substituted by fixed elements, to increase the stability of the system; and finally (v) a new more efficient CCD, with a smaller pixel has been acquired.

CAFE is a stationary echelle spectrograph located at some remote laboratory in the dome building. Such room is located below the main telescope structure in a separated part of the rest of the building providing it with isolation of any mechanical vibration. Therefore the instrument is separated $\sim$18m from the Cassegrain focus of the telescope. A sophisticated pneumatic stabilization system is installed below the optical bench. This guarantees a much better stability of the instrument, increasing its performance and accuracy for velocity measurements of fainter objects.

The broad reinforced concrete walls also provide an thermal-isolation to the CAFE's room. Moreover, the spectrograph is inside a controlled thermal environment. Any thermal drifts of the instrument during an observing night due to temperature changes in the dome is avoided. The spectrograph can be isolated, first by holding the temperature in the laboratory constant, and second by enclosing the instrument in a methacrylate cabinet (Figure 1, left panel), covered internally by a layer of neoprene with 10mm of width. The upper part of the cabinet might be lift up with a tackle anchored on the roof of the room for getting access to the optical bench, as shown if figure 1, right panel.

Figure 1: Left panel: The figure shows an external view of an CAFE spectrograph. The instrument is housed in a thermal isolated cabinet. Right panel: The figure shows a view of an CAFE spectrograph with the cabinet opened. The internal optical elements can be watched on the optical bench. The upper size is as straight as a die to avoid any small apertures that can break the thermal isolation. Because of that, the upper part has to be lift up with the help of a tackle.

A latter control of any internal device is unnecessary once the instrument is integrated. Comparing with FOCES, some of the encoders and motors have been eliminated from the design, as the control of the grating angle, and the control of the prism relative angle. This parameters can be modified by a manual stage and later every optical mount is fixed permanetely, so the possibility of motion is void. Consequently the heat produced by such elements is eliminated. The only active elements inside the cabinet are the focus stage of the camera and the shutter, but both are disabled during the normal operation. Moreover, the removal of the movable parts in the optical path guaranties the stability of the mechanical mounts installed on the optical bench. Following the same philosophy, the entrance slit of the spectrograph is fixed to 100 μm.

The optical design of CAFE follows a white pupil design in near-Littrow mode that has been documented by Baranne (1998). The optical layout is shown in figure 2. Initially the light is collected by the telescope module that it is attached to the Cassegrain focus of the telescope. It contains a fibre positioning unit carries the fibre head plug and the entrance diaphragm which has circular aperture of 200 μm (2.4arcseconds). The proper position of the object can be observed by the light reflected from the entrance diaphragm using the telescope guiding facility.

A calibration mirror is mounted on a rotating stage and controlled by motor drives. It can be moved in and out of the object field receiving light from either calibration light source available. A new electronics control has been designed based on Peripheral Interface Controller (PICmicro).

There are two calibration lamps, the halogen flat field lamp and the ThAr calibration lamp) that are mounted at 90 degrees distance around the main body of the module. Their light passes through a diffusor and is focussed on the entrance aperture where a 100 μm optical fiber collects the light and feeds the echelle spectrograph.

The first element in the optical bench is the entrance slit used to recover resolution if the entrance diaphragm at Cassegrain focus is wide open to pass starlight even in case of bad seeing. It is immediately aside of the folding mirror so the entrance slit and its spectral image are therefore very near together.

To follow a white pupil design, the spectrograph itself is collimated with two large off-axis parabolic mirrors. The 15 cm beam leaving the 31.6 lines/mm R2 echelle is refocussed in the vicinity of a small folding mirror, used to reflect the converging beam in the vicinity of the intermediate slit image which passes a very efficient straylight baffle.

The cross-dispersion is achieved with two LF5 prisms installed on a symmetric tandem mounting which is under manual control. Instead of a low-order grating, a double prism for cross-dispersion is used, which accounts for a less strongly changing inter order distance, and it significantly reduces local straylight in the spectrum.

Finally, the beam is imaged with an f3 transmission camera onto a field centered on a back-illuminated CCD with 13.5 μm pixel size. The optical design of the camera of the instrument has been optimized, based on the knowledgement acquired with FOCES. The efficiency of the instrument is at least a 10% due this new optimized design CAFE.
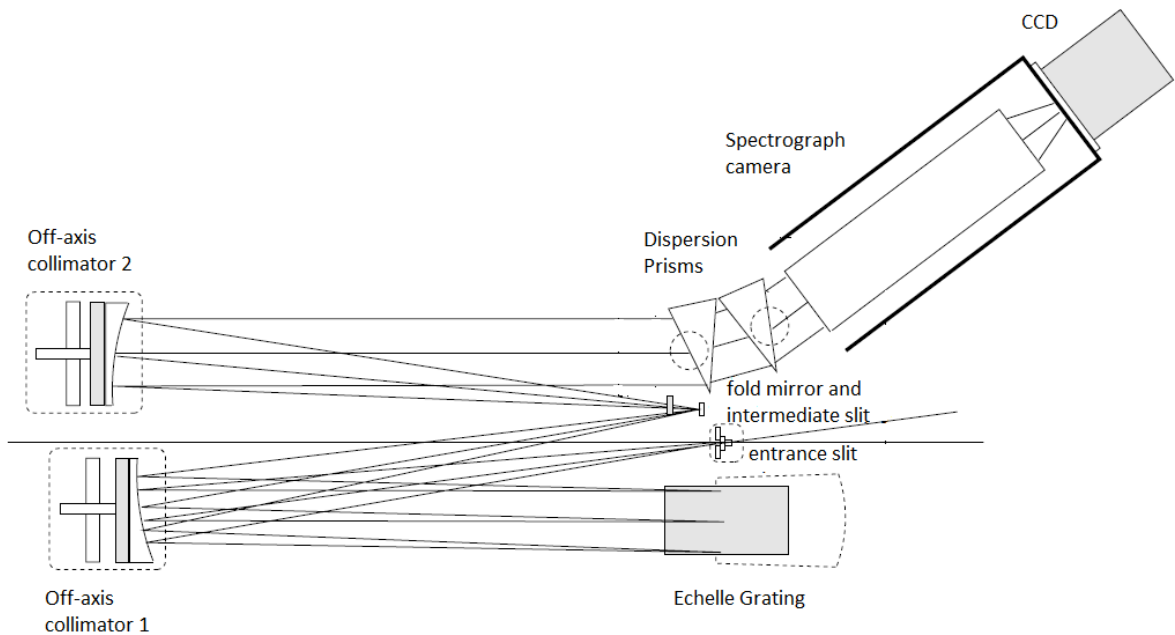
Figure 2: The figure shows a view of an CAFE spectrograph with the cabinet opened. The internal optical elements can be watched on the optical bench. The upper size is as straight as a die to avoid any small apertures that can break the thermal isolation. Because of that, the upper part has to be lift up with the help of a tackle.

3   CCD Characterization

The CAFE detector is a commercial CCD from Andor TechnologiesÃOA model iKon-L 936. The 2048 x 2048 array and 13.5 x 13.5 μm pixels combine to deliver a 27.6 x 27.6 mm active image area.

iKon-L boasts a proprietary large area 5-stage termo-electric cooler, enabling cooling of the large area sensor down to an -90r̈C helped with a water-cooling system model Oasis 150. The Oasis 150 is a thermoelectric temperature control system with full PID control of both heating and cooling. It provides 500 ml/min of constant temperature coolant for controlling the operating temperatures of the CCD. It does not use Freon or any other replacement gas, so there is no aggravation of liquid nitrogen or compressed gas cooling.

USB 2.0 connectivity provide an ease integration and operation in a PC. Multi-MHz readout options are available from slower readout for low noise, or faster speeds for dynamic processes as focus mode.

The main features of the CCD are summarized in the table 2.

The quantum efficiency of the detector is shown in figure 3. The peak value is 95% at 550nm. This is almost a 10% better than the quantum efficiency of the detector normally used together with FOCES, LOR#11i that got a highest value of 85% at 500nm.

3.1   Bias stability.

In order to check the stability of the bias along the time, a series of dark frames with different integrations times has been taken. The exposure times were in a range from 1 to 4000 seconds per frame. The test was completed in 5 hours and the results are plotted in the figure 4, where the median of the frame is plotted versus the exposure time. The dark current has been corrected according to integration time. The results shows no tendency of the bias level and a very stable pattern through this time.

Table 2: Main features of CAFE's detector

Sensor	Back Illuminated CCD, Vis optimized
Active pixels	2048x2048
Pixels size	13.5 x 13.5 μm
Image area	27.6 x 27.6 mm with 100% fill factor
Water cooled	-90 žC
Blemish specification	Grade 1 sensor
System window type	Single quartz window wit AR coated on both sides
Pixel readout rates	5, 3, 1, 0.05 Mhz
Pixel well depth	100000 e-
Digitization	16 bit
Vertical clock speed	38 or 76 μs
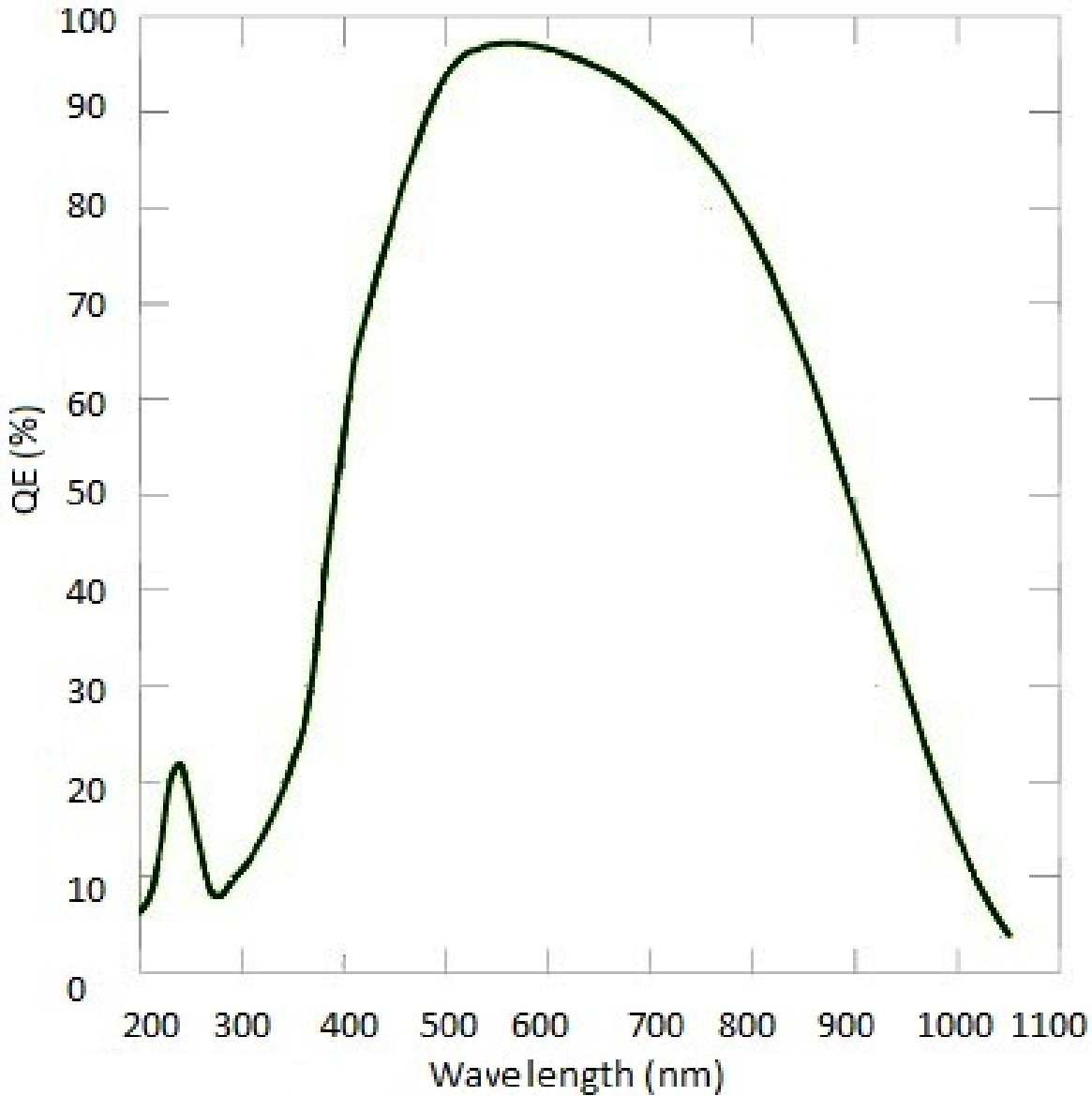
Figure 3: Quantum efficiency of the detector IKON-L. It shows a peak value up to 95% at 550nm.
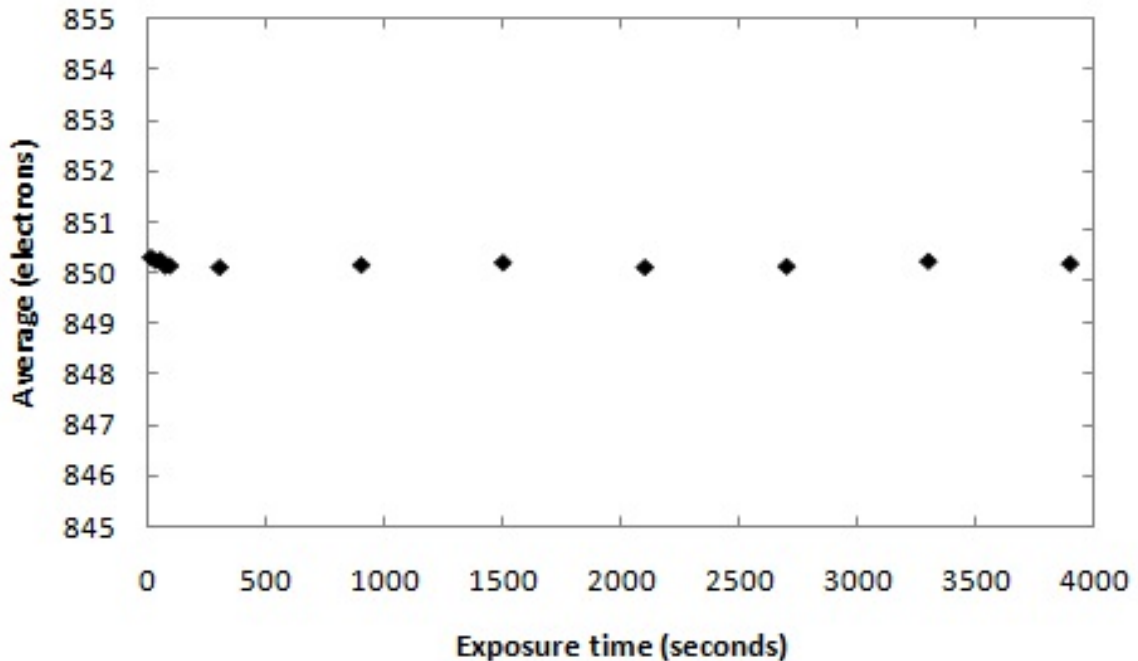
Figure 4: Stability of the bias level along the time. Every spot represents the mean value of a dark frame for a given exposure time. Previously comics rays have been removed by combining three frames in median.

Table 3: Dark current for different working temperatures[a]

CCDTemp (žC)	e-/pixel/sec
-70	0.0004
-80	0.00018
-90	0.00015

[a]Dark current measurement is taken as a median over the sensor area excluding any regions of blemishes.

3.2 Dark current and readout noise.

Dark current and readout noise have been calculated for the CCD. To do that, as in the previous test, a series of dark frames with different exposure times have been taken.

Figure 5 shows the plot of the standard deviation versus the exposure time of the dark frame at different exposure times. The value obtained for zero seconds of integration time means the readout noise. A linear tendency might be fitted to the experimental data providing information about the dark current (0.000154e-/pixel/sec) and the readout noise (2.53e-). These data were computed for the standard setup of the CCD (i.e. Readout rate = 50Khz, gain = 1.0e-/ADU, CCD temperature = -90žC). Other values of the dark current obtained for different temperatures of the detector are shown in table 3.

Currently there are different observing modes that can be selected depending of the output of the AD channels of the CCD and the readout rate. By selecting the output of the AD channels, a high sensitivity or high capacity modes can be selected. The first one is recommended for low-light applications while the second one is used to get the maximum dynamic range.

The readout noises for all these modes related to the frame rates and pre-amplifier gains available are shown in table 4 and 5. Readout noise is computed for the entire system. It is a combination of sensor readout noise and A/D noise. Measurement is for single pixel readout with the sensor at a temperature of -90řC.

Depending of the readout rate selected, the readout time can vary from 6 second to 90 seconds. Faster readout rates have an impact on higher readout noise. The recommended setup during the observations will be 0.05Mhz and high sensitivity mode. Other duties as the focus tasks can be done with faster rates as 5.0Mhz and the
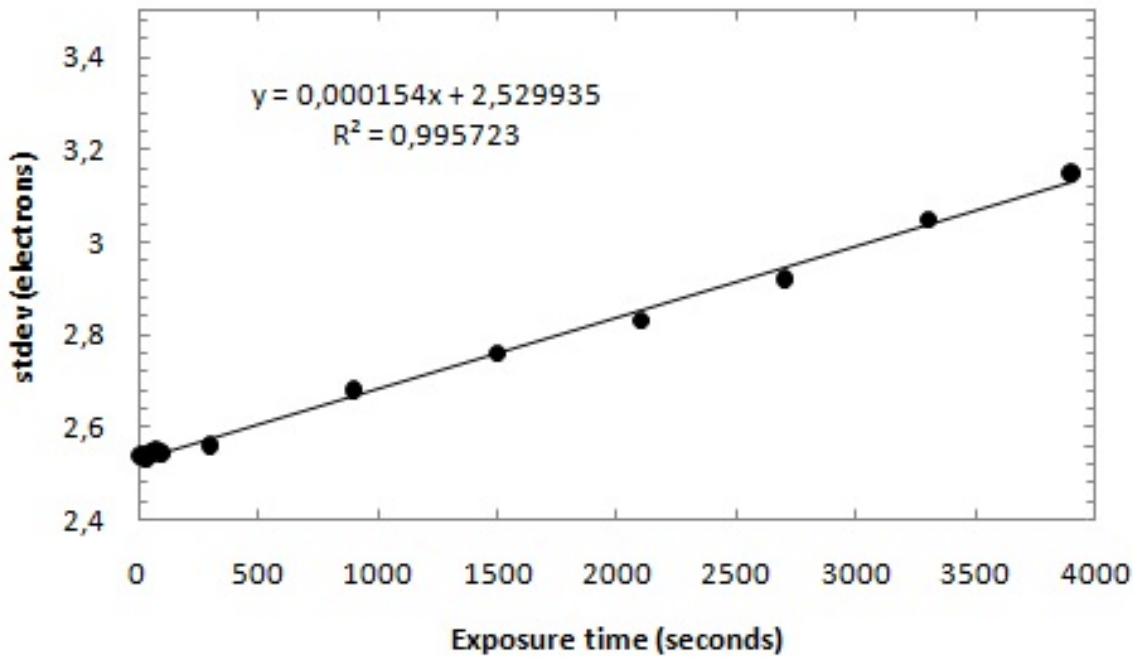
Figure 5: Dark and readout noise.

high sensitivity mode.

3.3 Linearity

The linearity of the detector has been characterized by taking a series of images with a constant illumination and varying the exposure time to get signals from very low levels up to saturation that occurs at 65535 counts. Figure 6 shows the deviation of the experimental data respect to the expected lineal dependency of the exposure time and the signal level.

The deviation is expressed as a percentage and is better than 0.5% if the signal is below 42000 counts, better than 1.0% if the signal is below than 48000 counts and better than 5% if the signal is below than 55000 counts.

This test has been carried out only for the recommended observing mode (i.e. 0.05Mhz and high sensitivity mode, -90žC). Faster readout modes will decrease the linearity range of the detector and should be taken into account.

3.4 Fringing

The thickness of the substrate silicon used in standard back-illuminated CCD sensors such the CAFE CCD tends to be <20ţm. Long wavelength photons >600nm can pass through the silicon and be reflected. These reflections between the parallel front and back surfaces of the sensor can lead to unwanted fringes of constructive and destructive interference. This resonant effect causes the device to become semi-transparent in the near-infrared region of the spectrum. The effect increases at longer wavelengths which is why the effect is more noticeable in the red region on the spectrum.

The new CCD has a tremendous fringing that seems to be scaring. In the figure 7, a continuum exposure (raw frames) is compared with a master continuum exposure (combination of one night, i.e., 10 frames), and the ratio between both plots. The ratio between both figures shows a standard deviation of just 2%.

By adopting the same scheme as used in fiber-transmission correction for other instruments, it is feasible to correct for the fringing. Figure 8 shows a comparison of one of the orders more heavily affected by this effect,

Table 4: High Sensitivity mode

Rate (Mhz)	Gain (e-/ADU)	Pixel noise (e-)	Bias level (counts)	Readout time (sec)
5.0	8.9	75.8	2236	6
5.0	4.1	49.4	3432	6
5.0	2.2	34.6	5218	6 [a]
3.0	3.6	29.1	1367	8
3.0	2.0	16.0	1843	8
3.0	1.0	12.5	2279	8
1.0	3.5	9.8	820	10
1.0	1.8	7.0	843	10
1.0	1.0	6.6	855	10
0.05	3.4	3.8	828	90
0.05	1.8	2.9	836	90
0.05	1.0	2.6	850	90[b]

[a]Recommended mode for focus tests.
[b]Recommended mode for observations.

Table 5: High Capacity mode

Rate (Mhz)	Gain (e-/ADU)	Pixel noise (e-)	Bias level (counts)
5.0	10.5	79.4	926
5.0	8.9	81.3	921
5.0	6.0	73.3	945
3.0	14.6	112.3	843
3.0	7.7	64.9	993
3.0	4.1	45.8	1127
1.0	14.6	40.7	832
1.0	7.4	26.0	864
1.0	3.8	23.2	907
0.05	15.1	14.3	842
0.05	7.5	9.7	861
0.05	4.0	8.6	896
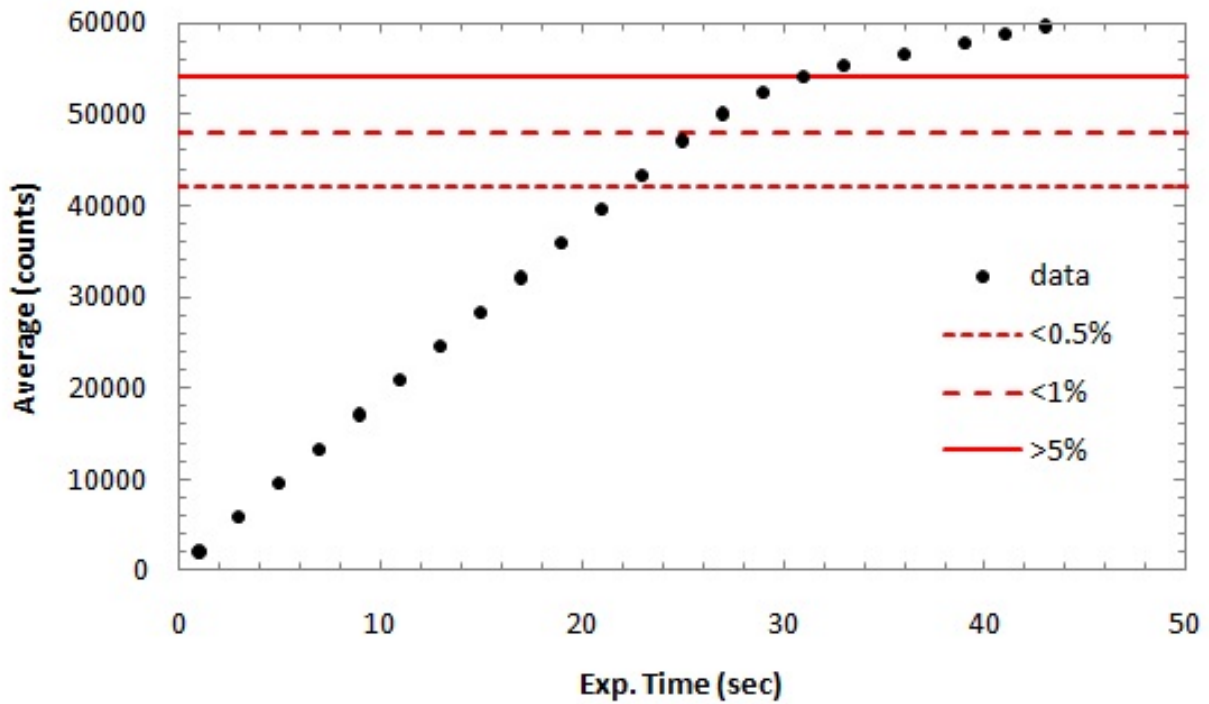
Figure 6: Linearity behavior of the detector of CAFE. The horizontal lines represent the percentage deviation of the experimental data respect to the ideal dependency of the signal level versus the exposure time.
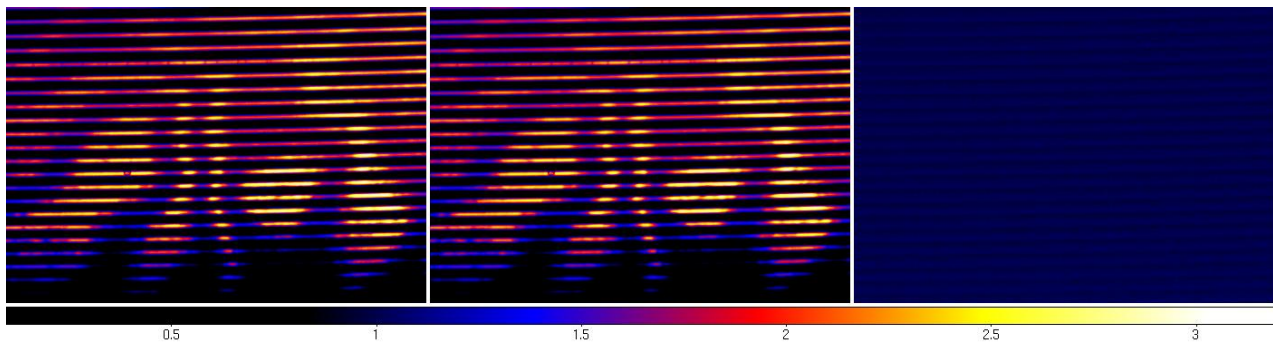
Figure 7: Fringing pattern of the CAFE detector. Left panel: raw image, center panel: master continuum exposure, right panel: ratio between both.
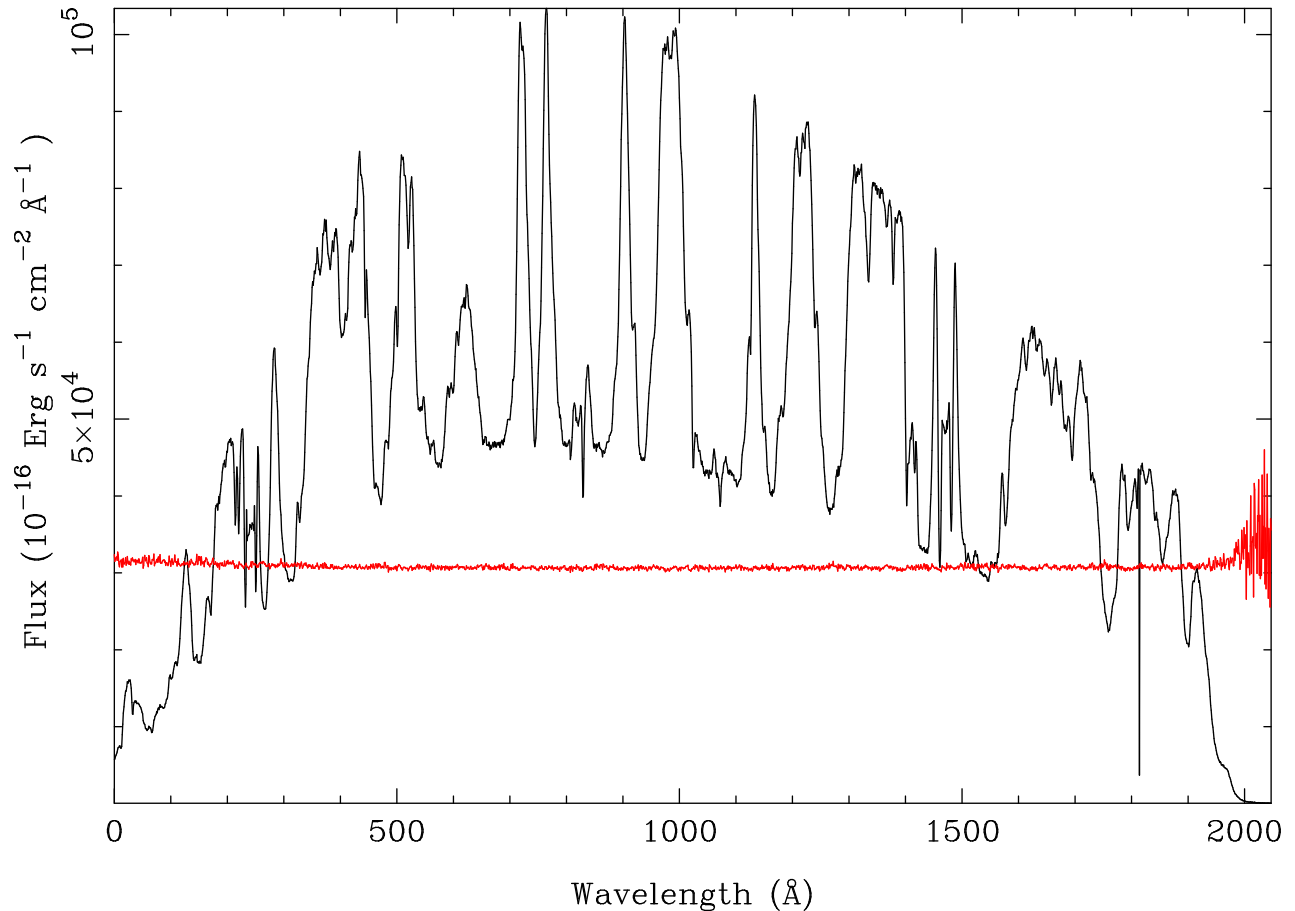
Figure 8: The figure displays a plot of an order heavily affected by the fringing. Black line represents the order before the corrections and red one after the corrections.

before and after the correction. The current implemented correction has an accuracy of 1.2%. A master-flat has been created to handle this effect.

4   First Light

The first light of CAFE tooks place the night of the 16th of May 2010, when the instrument was for the first time installed in the telescope, and tests were performed during the night.

The main goals of this first light were:

- Test the acquisition software.

- Test the centroiding on fiber/Guiding system. Acquire light from astronomical targets.

- Describe the raw data (orders/wavelength/projection in the CCD) and prepare the first tentative data reduction.

- Test qualitatively the efficiency of the system.

- Test the overall performance of the system.

All the goals were achieved during the night. Several different bugs and glitches were detected in the acquisition software, and in particular a problem when using the lower RON read-out system (VALUE?). The problems were solved during the subsequent days before the commissioning.

Table 6 summarizes the observing log during the first light of CAFE, including the hour of the observation, the name/type of target and the exposure time. As it can be seen we took a continuum and arc frame (ThAr)
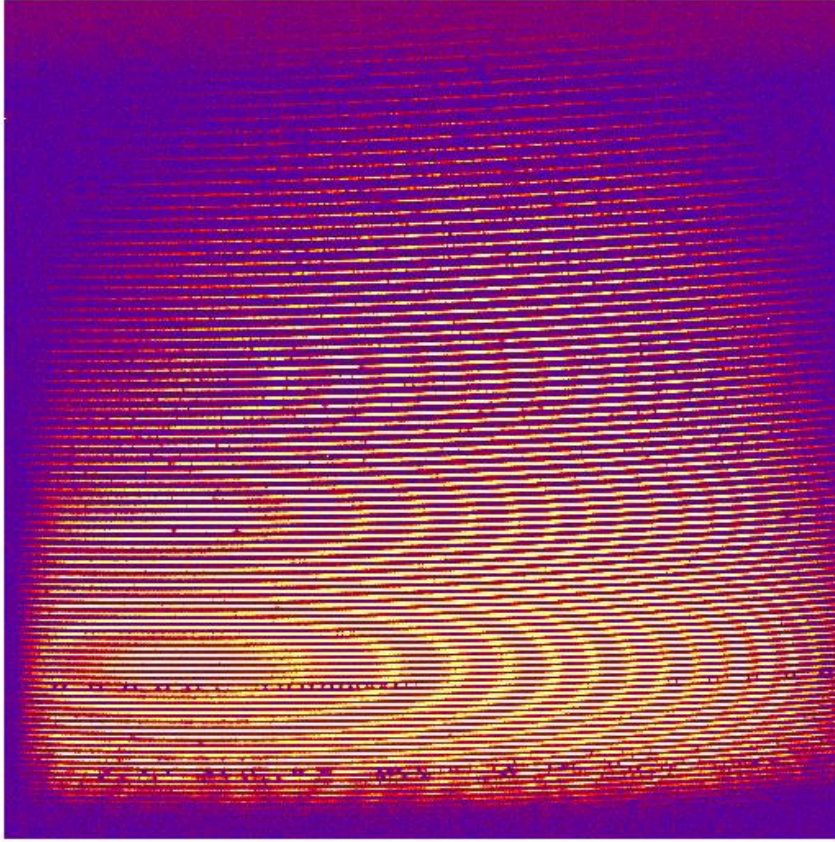
Figure 9: Raw data of the first science frame taken with CAFE, on the star HR4728.. The orders are displayed from red, at the bottom, to blue, a the top. For each order, the wavelength range runs from blue, at the left, to red, at the right.

Table 6: Log of the First Observing night

Time	Object Name	Exposure Time (sec)
2011-05-05T 18:25:25 temporal	BD+26 2606	300
2011-05-05T 18:25:25 temporal	Bias	0
2011-05-05T 18:25:25 temporal	Cont	10
2011-05-05T 18:25:25 temporal	Bias	0
2011-05-05T 18:25:25 temporal	Bias	0
2011-05-05T 18:25:25 temporal	Bias	0
2011-05-05T 18:25:25 temporal	ThAr	30
2011-05-05T 18:25:25 temporal	Cont	20
2011-05-05T 18:25:25 temporal	Cont	5
2011-05-05T 18:25:25 temporal	HR4728	5
2011-05-05T 18:25:25 temporal	HR4728	5
2011-05-05T 18:25:25 temporal	Tres-3	1800
2011-05-05T 18:25:25 temporal	ThAr	40
2011-05-05T 18:25:25 temporal	Cont	10
2011-05-05T 18:25:25 temporal	Saturn	100
2011-05-05T 18:25:25 temporal	Saturn	100
2011-05-05T 18:25:25 temporal	Saturn	100
2011-05-05T 18:25:25 temporal	Saturn	100
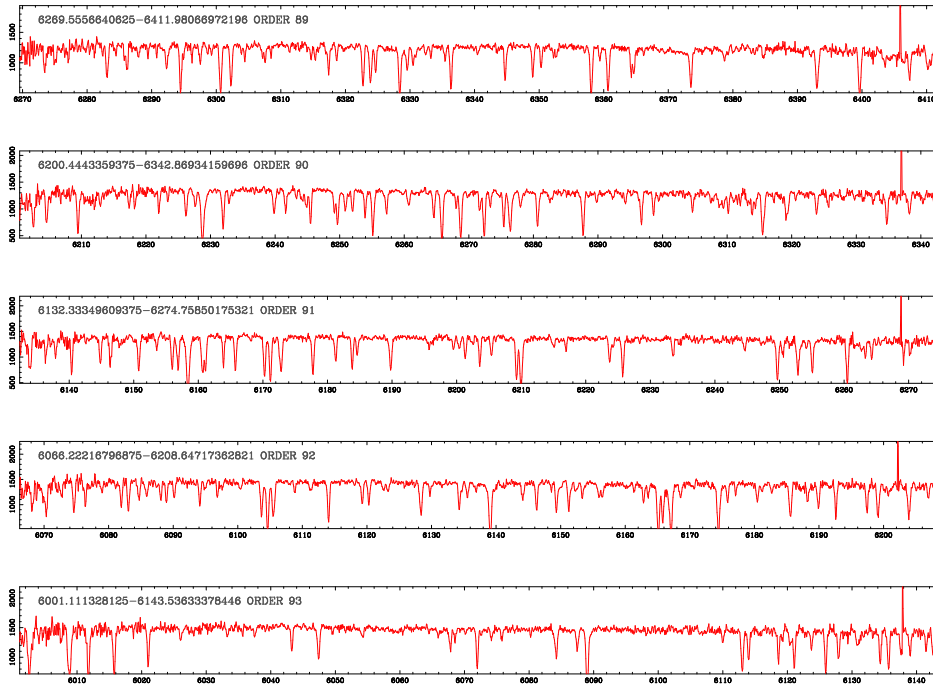
Figure 10: Detail of a few orders of the extracted spectra of HR4728, reduced using the early version of the pipeline.

just prior to any science frame during the night. This was done in propose to estimate the stability location spectra projected in the CCD, and to trace any possible change on the focus with the monitored parameteres (e.g., the temperature).

The first observed science target was a bright ($V \sim 6$ mag) star, HR4728, selected by visibility and luminosity to ensure that it is well centred in the fiber an easily identified in the raw data. A short exposure of 5 seconds was taken, as a tentative guess, since we ignore so far the final performance of the instrument. A S/N$\sim$30 was derived in a rough way by comparing the integrated flux at the peak intensity with the background noise. So far, this S/N does match with our initial expectations of the performance of the instrument.

4.0.1 Identification of the orders

The early tests performed along this night on the data were focused on the identification of the orders and wavelength range covered by each order. The identification of the orders was a fundamental and not trivial task prior to the proper extraction and wavelength calibration of each frame.

First, the location of the projection of each order in the CCD, as seeing in images 9 is determined using the corresponding tracing routines. Figure 11 shows a vertical cut of continuum lamp exposure used to trace these locations, showing the distribution of flux along the cross-dispersion axis corresponding to each of the orders. For each order, the location of the peak intensity is indicated with a red (central pixel) and blue (centroid) cross.

The identification of the orders was done after tracing and extracting a ThAr fram (following the reduction steps explained in the Appendix I). Each emission arc spectra was then compared with a similar one from FOCES. The first result found was that the wavelength range covered by each order and the identified orders is slightly different between FOCES (REF) and CAFE, being the wavelength range slighy shifted to the red.

Table 7 shows the 84 detected orders, including the Y-coordinate of the peak intensity of each order projected in the CCD at the central pixel in the X-axis, i.e., the pixel marked with a red cross in Figure 11. Table 8 shows, for each order, the wavelength range sampling, once normalized to a common spectral sampling per pixel.
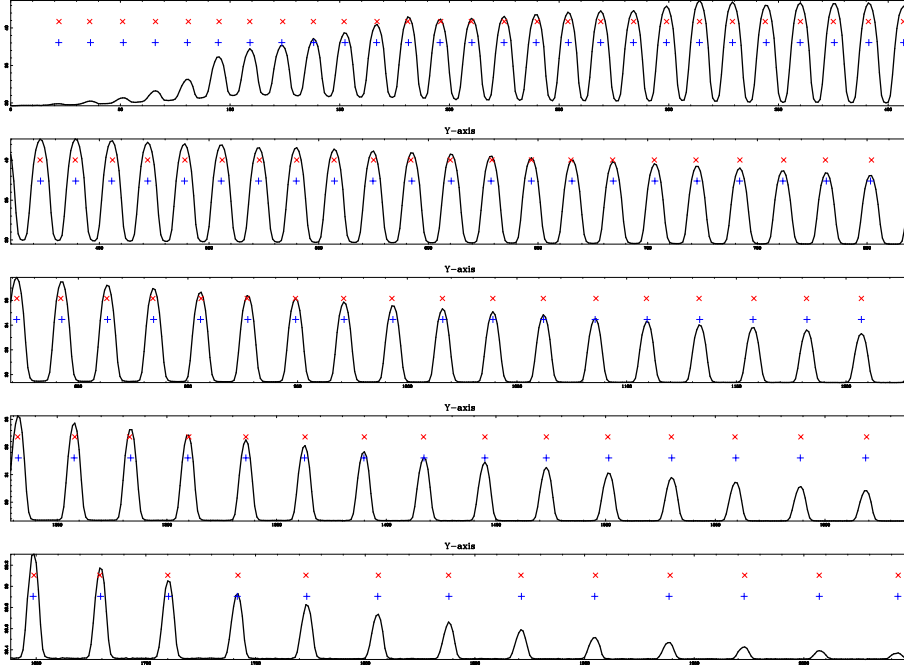
Figure 11: Vertical section of a continuum exposure at the central X-axis pixel, showing the projection on the CCD of each order, from red wavelengths (top-left) to blue ones (bottom-right). The location of the peak intensity of each order is marked with a red cross (central pixel), and with a blue cross (centroid).

5   Commissioning

5.0.2   Efficiency of the Instrument

The net efficiency of the instrument was derived by comparing the expected photons to obtain from a certain source with the real number of photons acquired by the instrument. For doing so, it was used the exposures on the calibration stars during the night of the 17th of July 2011. These nights we observe 5 different calibraion stars along the night. These exposures were reduced using the procedures described in the Appendix, and finnally it was derived a (flux) uncalibrated spectra for each of the orders, in counts. Then, counts 2were transformed to photoelectron using the gain of the CCD. For each wavelength, this gives us the number of detected photoelectrons ($n_{e,det}$).

To derive the number of expected photoelectrons it is required to use the known flux-calibrated spectra of the considered standard stars. There stars were all extracted from the Oke (1990) catalogue [3], which flux density is provided in units of 10^{-16} Erg s^{-1} Å^{-1} cm^{-2}. The amount of flux (F) at a certain wavelength λ, in a wavelength interval $\Delta\lambda$, of a star (or any other target), with flux density f_λ, collected by a telescope of collecting area (ΔS), in a time interval (Δt) is given by the formula:

$$F = f_\lambda \cdot \Delta S \cdot \Delta t \cdot \Delta\lambda$$

On the other hand, the energy of a single photon will be:

$$f_{photon} = \frac{hc}{\lambda}$$

The ratio between both quantities, gives the number of *expected* photoelectrons ($n_{e,exp}$). This number can be compared directly with the number of *detected* photoelectrons, obtained from the reduced data as described before, to obtain the net efficiency of the instrument. E.g.,

---

[3]http://www.caha.es/pedraz/SSS/Oke/oke.html

Table 7: CAFE: List of clearly detected orders, including, for each order, the Y-coordinate of the pixel of the peak intensity of the projection in the CCD, at the central pixel in the X-axis.

#	Y pixel	#	Y pixel	#	Y pixel [*]
60	152	88	593	116	1182
61	167	89	611	117	1207
62	181	90	629	118	1232
63	196	91	647	119	1258
64	210	92	666	120	1283
65	225	93	685	121	1310
66	240	94	703	122	1336
67	254	95	723	123	1363
68	269	96	742	124	1390
69	284	97	762	125	1417
70	299	98	782	126	1445
71	314	99	802	127	1473
72	329	100	822	128	1501
73	345	101	843	129	1530
74	360	102	864	130	1559
75	376	103	884	131	1589
76	391	104	906	132	1618
77	407	105	927	133	1649
78	423	106	949	134	1679
79	439	107	971	135	1710
80	456	108	994	136	1741
81	472	109	1016	137	1773
82	489	110	1039	138	1805
83	506	111	1062	139	1837
84	523	112	1086	140	1870
85	540	113	1109	141	1905
86	557	114	1133	142	1938
87	575	115	1158	143	1972

$$efficiency = \frac{n_{e,det}}{n_{e,exp}}$$

Figure 12 shows the derived efficiency of the instrument (+telescope+detector), as a function of the wavelength. CAFE seems to be singnificantly more efficient than FOCES, at any wavelength range (REF/priv. communications). Comparing with similar Echelle instruments, avaiable in telescopes of a similar size, CAFE has a similar peak efficiency as FEROS (REF/WEBPAGE), although this instrument is more efficient in the blue end. The main different seems to be the efficiency of the CCD, which for FEROS has a coating which efficiency change from blue to red from one side to another across the CCD (REF).

A possible way to improve the efficiency of the instrument would be to change the CCD.

5.0.3 Instrumental Focus and Wavelength Resolution

One of the main goal when designed (and build) CAFE was to achieve a better resolution than the one FOCES and reach, or at least, reach a the best resolution that that instrument could offer (with a better efficiency and stability). CAFE was designed to achive a maximum resolution of $R \sim 70000$ (Sánchez et al. 2007), in the optimal situation.

The resolution of the instrument is defined as the ratio between the wavelength λ and the minimum range of wavelegths that can be resolved $\Delta\lambda$. In practice, $\Delta\lambda$ is derived from the FWHM, in the spetral direction, of the emission lines of ARC lamps. Assuming that these lines are (in general), unresolved, the FWHM measures the instrumental resolution, i.e., the minimum wavelength elements to be resolved. Early measurements in the Lab. indicate that the FWHM of these emission lines were around ~ 2.2 pixels, which mostly corresponds to a R$\sim$67000 at the average wavelength sampled by the instrument ($\lambda 6500$Å).
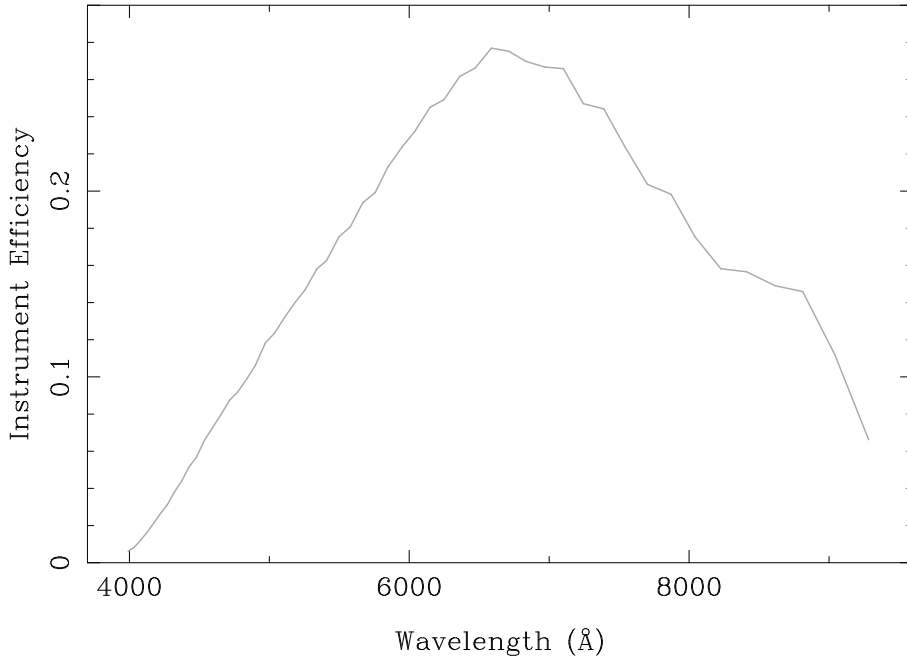
Figure 12: CAFE Efficiency curve
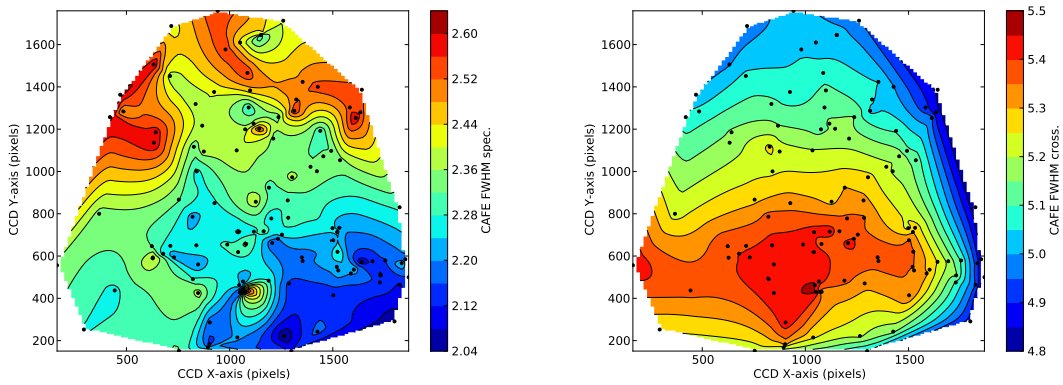
Figure 13: CAFE: FWHM of the ARC emission lines. Left panel shows the distribution of the FWHM of the ARC emission lines along the dispersion axis (X-axis), across the field-of-view of the CCD. Right panel shows a similar distribution for the FWHM along the cross-dispersion axis.

Table 8: CAFE: List of the clearly detected orders, including the order, the wavelength range and the spectral sampling (after resampling).

#	λ_{start} (Å)	λ_{end} (Å)	$\Delta\lambda/pix$ (Å/pix)	#	λ_{start} (Å)	λ_{end} (Å)	$\Delta\lambda/pix$ (Å/pix)	#	λ_{start} (Å)	λ_{end} (Å)	$\Delta\lambda/pix$ (Å/pix)
60	9432.964	9558.496	0.0645	88	6430.853	6516.885	0.0442	116	4877.880	4943.502	0.0337
61	9278.291	9401.792	0.0634	89	6358.568	6443.648	0.0437	117	4836.160	4901.236	0.0334
62	9128.607	9250.142	0.0624	90	6287.889	6372.039	0.0432	118	4795.146	4859.686	0.0331
63	8983.674	9103.305	0.0614	91	6218.764	6302.003	0.0427	119	4754.821	4818.833	0.0328
64	8843.271	8961.057	0.0605	92	6151.141	6233.490	0.0423	120	4715.168	4778.662	0.0326
65	8707.188	8823.185	0.0596	93	6084.972	6166.449	0.0418	121	4676.170	4739.154	0.0323
66	8575.229	8689.491	0.0587	94	6020.210	6100.835	0.0414	122	4637.811	4700.294	0.0321
67	8447.208	8559.787	0.0578	95	5956.812	6036.603	0.0410	123	4600.075	4662.066	0.0318
68	8322.953	8433.897	0.0570	96	5894.734	5973.708	0.0405	124	4562.947	4624.454	0.0316
69	8202.299	8311.657	0.0561	97	5833.936	5912.109	0.0401	125	4526.413	4587.443	0.0313
70	8085.092	8192.908	0.0554	98	5774.378	5851.768	0.0397	126	4490.459	4551.020	0.0311
71	7971.187	8077.504	0.0546	99	5716.023	5792.646	0.0393	127	4455.070	4515.170	0.0308
72	7860.446	7965.305	0.0538	100	5658.835	5734.706	0.0389	128	4420.234	4479.881	0.0306
73	7752.738	7856.180	0.0531	101	5602.779	5677.913	0.0386	129	4385.938	4445.138	0.0304
74	7647.942	7750.003	0.0524	102	5547.822	5622.233	0.0382	130	4352.168	4410.929	0.0301
75	7545.939	7646.658	0.0517	103	5493.932	5567.634	0.0378	131	4318.914	4377.243	0.0299
76	7446.621	7546.032	0.0510	104	5441.077	5514.086	0.0375	132	4286.164	4344.066	0.0297
77	7349.883	7448.020	0.0504	105	5389.229	5461.557	0.0371	133	4253.905	4311.388	0.0295
78	7255.624	7352.520	0.0497	106	5338.359	5410.019	0.0368	134	4222.128	4279.198	0.0293
79	7163.752	7259.438	0.0491	107	5288.440	5359.444	0.0364	135	4190.821	4247.485	0.0291
80	7074.176	7168.682	0.0485	108	5239.445	5309.805	0.0361	136	4159.974	4216.237	0.0289
81	6986.812	7080.168	0.0479	109	5191.348	5261.078	0.0358	137	4129.577	4185.446	0.0287
82	6901.579	6993.811	0.0473	110	5144.125	5213.236	0.0355	138	4099.620	4155.101	0.0285
83	6818.399	6909.536	0.0468	111	5097.753	5166.255	0.0352	139	4070.093	4125.192	0.0283
84	6737.199	6827.267	0.0462	112	5052.209	5120.114	0.0348	140	4040.988	4095.710	0.0281
85	6657.910	6746.933	0.0457	113	5007.470	5074.789	0.0345	141	4012.296	4066.645	0.0279
86	6580.464	6668.467	0.0452	114	4963.516	5030.259	0.0342	142	3984.007	4037.990	0.0277
87	6504.799	6591.805	0.0447	115	4920.326	4986.504	0.0340	143	3956.113	4009.736	0.0275

A detailed derivation of the spectral resolution can be done done after a proper identification of the orders, the wavelength range covered by each of them, and the corresponding sampling ratio per pixel. Once reduced any ARC lamp exposure, using the pipeline described in the Appendix, each of the 336 identified arc emission lines are used to fit a Gaussian function in both the dispersion and cross-dispersion directions, deriving the FWHM in both axis. The FWHM in the cross-dispersion axis illustrate how well each order is separated form the adjacent ones, and by how amount they are contaminated by cross-talk. Figure 13 shows the distribution of both FWHMs across the field-of-view of the CCD.

NOTE: A procedure should be implemented to improve the flat-ness of both distributions, or, at least, the one along the dispersion axis. This will improve the image quality, at least in the spectra dispersion axis (X-axis)

On the other hand, the FWHM in the dispersion axis is a direct measurement of the spectral resolution. Once it is derived the FWHM of each of the indentified lines, a clipping algorithm rejects those vaules ($< 10\%$) that deviated more than 3σ of the mean value. The derived FWHM are multiplied by the step in wavlength per pixel and divided to the wavelength of the line, to derive the instrumental resolution (R).

Figure 14 shows the distribution of the spectral resolution along the wavelength derived from the first ThAr lamp observed the night of the 16th of June 2011. Similar distributions are found for any of the arc calibration frames taken along the Commisioning run. In average, the instrument resolution estimated on real data corresponds to $\sim63000 \pm 4000$ Å. There is a clear trend in the resolution from the blue to the red range, with the resolution being ~60000 in the blue end (~4000Å), and about ~70000 in the red end (~9500Å). This median value is statistically dominated by the values at wavelengths bluer than ~5500Å, where there are more
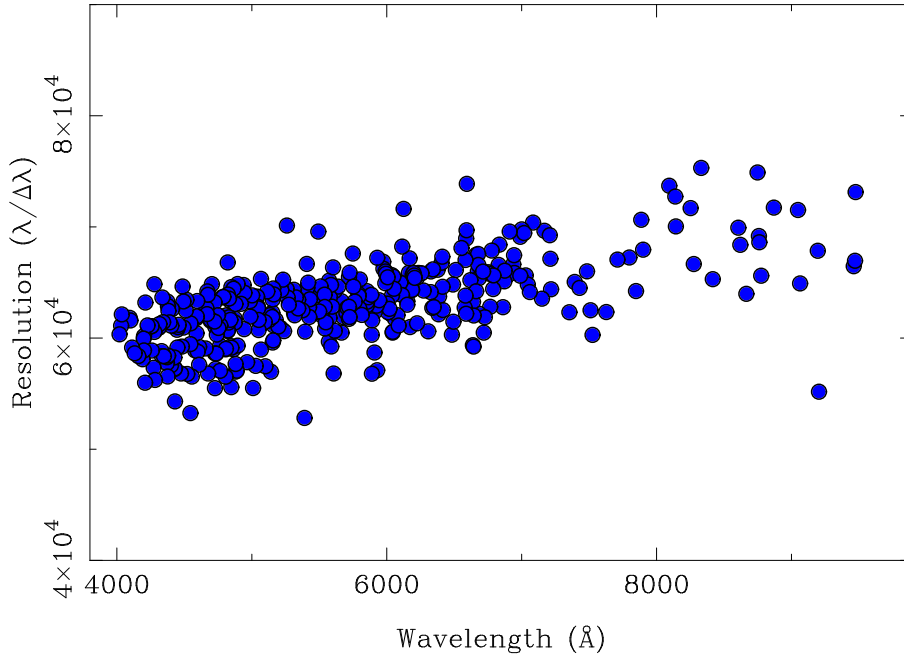
Figure 14: CAFE: Wavelength resolution derived from the estimation of the FWHM of the identified ARC emission lines in the dispersion axis.

identified arc lines. As anticipated, the resolution at the average wavelength of ~ 6500Å is ~ 65000 Å.

NOTE: Following the expecificatoins of the design, CAFE was build and calibrated to produce a similar accurate image quality at any position across the CCD. I.e., it was a goal of the design to have the same FWHM in the ThAr spots from blue to red amd at any order, at least in the spectral axis. A constant FWHM (in pixels) produce an unavoidable change in the resolution along the spectral range, as the one observed here.

This resolution is, in average, larger than the one that could be achieved by FOCES[4]. With that instrument, it was feasible to reach a resolution of about $\sim$65000 only when observing with the narrowest slit width (with the consequent lose of intensity), and it was not feasible to achieve a resolution well above this value.

NOTE: the estimation of the resolution of FOCES was done assuming a resolving power of 2 pixels, but no FWHM direct measuremnt was really done

5.0.4   Stability of the Focus

CAFE was designed to stabilize the focus (and therefore the resolution) as much as possible. Due to that, compared with FOCES, many moving elements has been replaced by fixed ones. To test if this goal has been achieved it is required to repeat the measurements described in Section for different ARC-lamps exposures taken under different conditions.

So far, we got 34 ThAr ARC lamp frames along the Commissioning run. We repeated the procedure described before for each of them, deriving the mean (and standard deviation) of the FWHMs values measured for each of them, and compated one each other. Figure 15 shows the distribution of these mean FWHMs along the time (left panel) and along the internal temperature of the instrument. It is important to note here than although the instrument is equiped with a thermal controlling system, this system was not operational during the Commissioning run. Therefore, any effect of the temperature on the focus (and the stability of the resolution) should be detected in this plot.

The average value of the FWHMs along the dispersion axis range between 2.3-2.35, without any significant variation either with the time and/or the temperature. The variation across the field is much larger (see Fig. 13 than any of possible detected variation along the time/temperature. In this regards, the goals of the design

---

[4]http//www.caha.es/pedraz/Foces/spec_resol.html
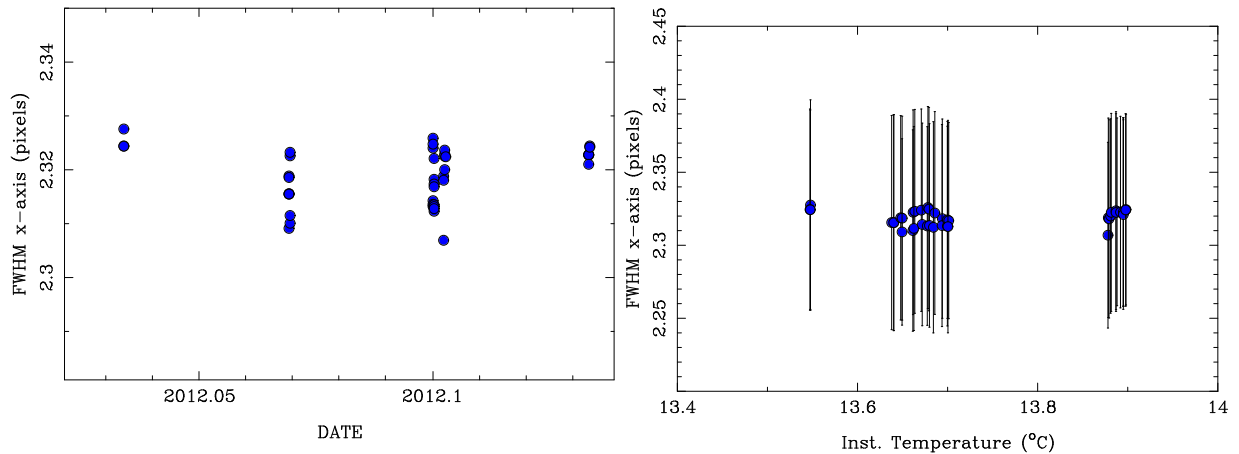
Figure 15: CAFE: Stability of the spectral resolution. Left panel shows the distribution of the average FWHM of the ARC emission lines along the dispersion axis (e.g., the one shown in Figure 14), for the different ARC frames taken along the commissioning run. Right panel shows a similar distribution along the internal temperature of the instrument, measured with the four sensors described in Section **??**.

has been completely ful-filled.

NOTE: It is required to (1) do this analysis for any of the observed nights here after to feed the statistics with more data, and (2) repeat the analysis if the focus is redo.

5.0.5 Signal-to-Noise

CAFE was designed to be fore efficient than FOCES. For doing so new branch fibers, optics, higher-efficiency elements and less movible elements were included. To determine if we have achieve this goal, we used the flux-calibrated spectra of the different objects observed during the commisioning run, and we derived the S/N ratio (per spectral pixel) on the basis of the variance provided by the Gaussian extraction included in the R3D (Sánchez et al. 2006).

NOTE: An automatic procedure to measure this S/N has been included in the CAFE pipeline.

Figure 16 shows two examples of the fully reduced spectra compared with their corresponding S/N for two targets, a bright radial velocity star ($V \sim 6$ mag), and the fainest target observed during the commissioning run, a faint star ($V \sim 14.5$ mag), both of them with similar spectral features at the considered wavelength range (order 97, $\lambda \sim 5850$Å).

Table 9 shows the results of this S/N analysis, for all the targets iobserved along the commisioning run, including the date, the name of the target, the V-band magnitude and the S/N at the average wavelength of this band (~ 5500Å). These results can be directly compared with the ones derived for FOCES[5]. We highlight here the results derived for the **G5** star with V-band magnitude of 6.9 mag, derived with FOCES, obtaining a S/N~ 41 for a exposure time of 60 sec. This can be compared with the result we obtain for HF151541, with CAFE, a $V \sim 7.1$ mag star, for which we obtain a S/N~ 68 for with a exposure time of 60 sec. The fainest object listed in the FOCES signal webpage, is a **0p** star with a luminosity of $V \sim 10.5$ mag, for which it was obtained a spectra with a S/N~ 25 with a exposure time of 600 seconds. A similar star, BD+25d4655, V~ 10.6 mag, was observed with CAFE, for which we obtained a spectrum with a S/N~ 45, for with a similar exposure time ($t_{exp} \sim 600$ sec).

In average, the S/N derived by CAFE is 2 times larger than the one derived with FOCES for targets with similar luminosity and using similar exposure time.

Figure 17 summarizes the results of this analysis, showing in two different representations the dependency of the S/N with the intrinsic brightness of the observed object and the adopted exposure time. Based on these results, the limiting magnitude of CAFE would ~ 15 mag, for a exposure time of 1 hour, with a S/N ratio of ~ 25. We consider that the goal of providing with an instrument more efficient than FOCES has been fulfilled.

---

[5]http://www.caha.es/pedraz/Foces/signal.html
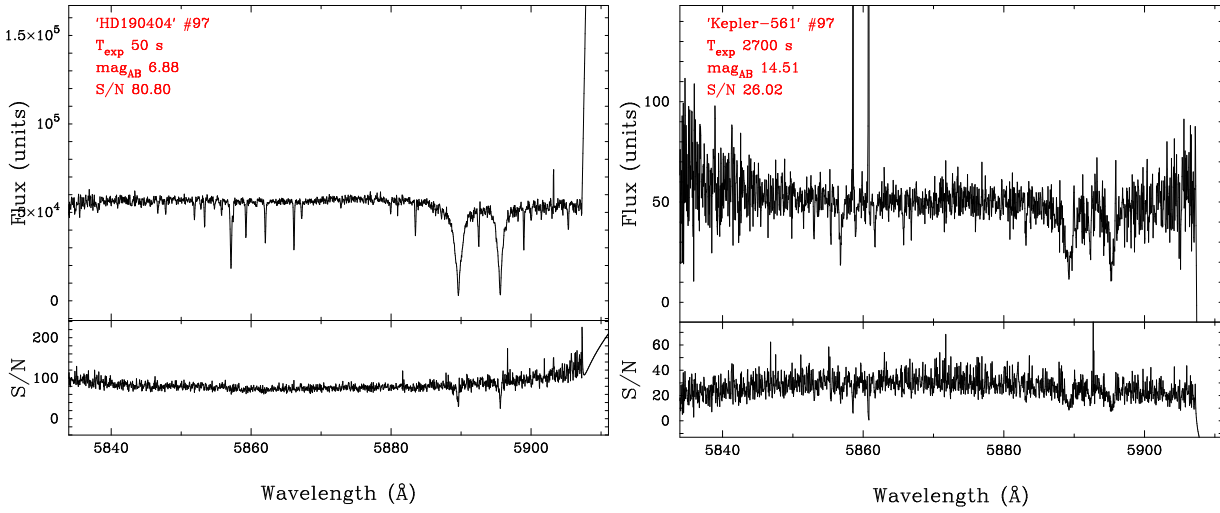
Figure 16: CAFE: Two examples of the spectra and S/N derived for a bright ($V \sim 7$ mag) and a faint ($V \sim 14.5$ mag) star, with similar spectral features at the considered wavelength range (order 97).
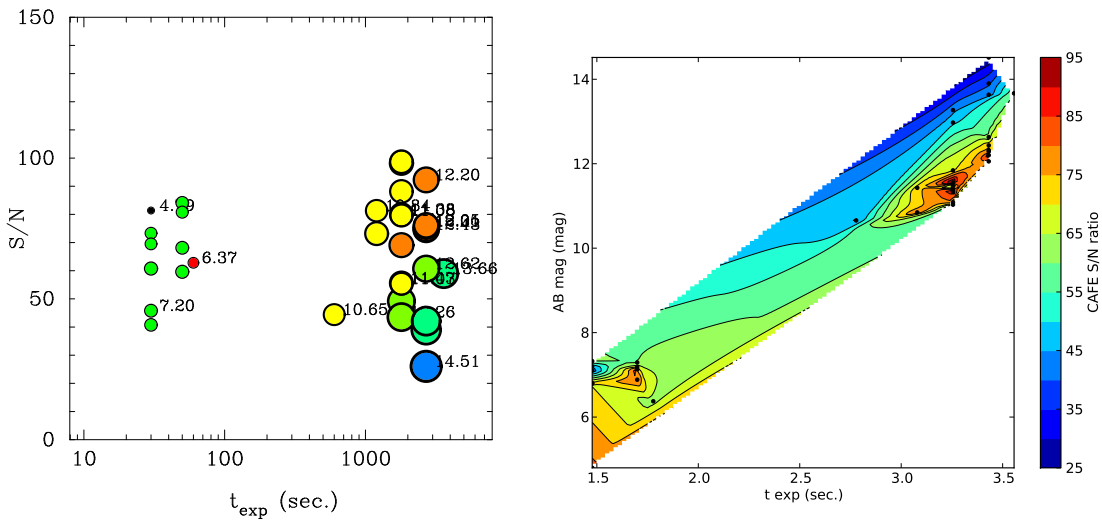
Figure 17: CAFE: Results from the analysis of the S/N. Left panel shows the distribution of the S/N along the exposure time, for the different observed objects. Color/size of the plotted symbols indicate the brightness of the considered object. Right panel shows the S/N distribution as a function of the brightness and the exposure time.

Table 9: Summary of the Observed objects along the Commissioning nights

Time	Object Name	Exposure Time	AB (mag)	S/N
11-06-15T22:30:10	HAT-P-12b	2700	12.4	74.6
11-06-15T23:22:36	WASP-24b	1800	11.3	88.1
11-06-16T00:29:44	KOI-561B	3600	13.6	58.9
11-06-16T00:45:04	HD154345	30	6.8	73.3
11-06-16T00:49:41	HD154345	60	6.3	62.8
11-06-16T01:27:21	Tres-2	1800	11.5	98.1
11-06-16T02:24:05	Tres-3b	2700	12.2	92.2
11-06-16T02:57:13	TrEs-2	1800	11.3	98.7
11-06-16T03:03:00	THD182572	30	4.7	81.3
11-06-17T21:13:45	HZ44	1800	11.8	69.0
11-06-17T21:46:51	Feige66	1200	10.8	81.3
11-06-17T22:14:10	BD+33d2642	1200	11.4	73.1
11-06-17T23:14:34	TrES-3b	2700	12.6	60.7
11-06-17T23:19:53	HD115404	30	6.7	69.5
11-06-17T23:35:51	HD139323	30	7.20	45.7
11-06-18T00:11:11	P330D	1800	12.9	49.1
11-06-18T00:52:22	TrES-2b	1800	11.4	55.6
11-06-18T01:04:29	HD151541	50	7.2	59.6
11-06-18T01:33:24	BD+25d4655	600	10.6	44.4
11-06-18T02:32:04	TrES-3b	2700	12.2	74.8
11-06-18T03:12:31	TrES-2b	1800	11.0	55.3
11-06-18T03:23:20	HD090404	50	7.1	84.1
11-06-18T20:58:34	P330D	1800	13.2	43.5
11-06-18T21:04:44	HD115404	30	7.1	40.7
11-06-18T22:03:56	TrES-3b	2700	12.3	75.7
11-06-18T23:00:47	Kepler-561	2700	13.8	39.0
11-06-18T23:35:28	TrES-2b	1800	11.3	79.9
11-06-18T23:44:03	HD139323	30	7.3	60.7
11-06-19T00:41:05	TrES-3b	2700	12.0	76.1
11-06-19T01:30:06	Kepler-561	2700	13.6	42.1
11-06-19T02:08:19	TrES-2b	1800	11.0	79.6
11-06-19T02:18:33	HD151541	50	7.1	68.1
11-06-19T03:12:25	Kepler-561	2700	14.5	26.0
11-06-19T03:25:07	HD190404	50	6.8	80.8

NOTE: These figures/tables should be fed with any additional information provided in any further observing run to derive much more accurate results/expectations.

6 Appendix

6.1 Appendix I: Pipeline

The actual pipeline of CAFE has been foreseen to allow the observer to make a quick&dirty reduction, visualize the data, and estimate the S/N of the data acquired at the telescope. It was not (initially) a goal to produce science useful datasets, although the accuracy of the reduction would allow their results to be used scientifically for some particular science cases.

The pipeline is based in R3D (Sánchez et al. 2006, [6]), and it is currently installed in CAHA computer named `r3dpipe`. The username required to access this computer is `r3duser` (password provided by CAHA staff).

There are two different set of scripts, one that reduces a single frame, and another that reduces all the science frames within a certain directory (labelled as `object`, in the `OBJECT` header keyword). These scripts are:

- `R3D_cafe.pl` (`R3D_cafe_SN.pl`). This script reduces a single frame. It requires three inputs: (1) the frame to reduce, (2) a continuum frame to trace the spectra of the differen orders projected in the CCD, and (3) an ARC-lamp frame used to identify the ARC emission lines and determine the wavelength calibration. This scripts creates two file, named after the prefix of the science frame, followed by the subfix `.disp_cor.fits`, which is the reduced frame (extracted, wavelength calbrated, and flat-fielded). It also produce a flux calibrated frame, named `.fc.fits`, which uses a master counts-flux flux-calibration transformation, derived during the commisioning run.

  This scripts uses also a master bias and a master flat field frame, created during the commisioning.

  The `*_SN.pl` scripts, provides with a SN-spectra, created on the basis of the propagation of the variance map derived by R3D. **NOTE: This latter script is slower**.

- `auto_redu_CAFE.pl` (`auto_redu_CAFE_SN.pl`). This script reduces all the object frames in a certain directory, by identifying them using the `OBJECT` header information, associating the required continuum and arc-lamp frames to each *science* frame, and applying the corresponding script described before.

Both scripts follow the basic procedures of the reduction of any fiber-fed spectrograph, described in Sánchez et al. (2006), that we will summarize here:

- Pre-reduction: The bias-level is subtracted from each frame using a master bias derived from the first observing nights. No CCDFlat or pixel-to-pixel correction has been applied so far.

- Order identification and extraction. The order identification and tracing is done using the routines included in R3D (`peak_find` and `trace_peaks_recursive`), by using continuum lamp exposures. A master flat frame is used by the pipeline. The extraction is performed using the Gaussian suppression extraction, assuming an average FWHM of the Gaussian functions along the cross-dispersion axis of $\sim$5.2Å(see Fig. 13. This extraction produce reduce effectively the effect of the cross-talk between different orders.

- Flat-fielding. The transmission through each order is different, and should be corrected to normalize it, on one hand, and to correct for the strong fringing effect detected in CCD. The transmission has a blue-to-red dependency that should be corrected prior to peform the flux calibration. This transmission drops at the edges of the CCD. **NOTE: TBD, determine the most useful wavelength range for each order, and trim the areas of lower S/N-transmission**. On the other hand, the fringing pattern has a dynamical range of $\sim$50% of the median flux for each order, and it is particularly strong in the redder ones.

  A Flat-field or order-transmission correction is created based on the reduced (traced and extracted) frame of a continuum illuminated exposure (so far, the continuum ARC-lamp). All the continuum ARC-lamp

---

[6]http://www.chaa.es/sanchez/r3d/
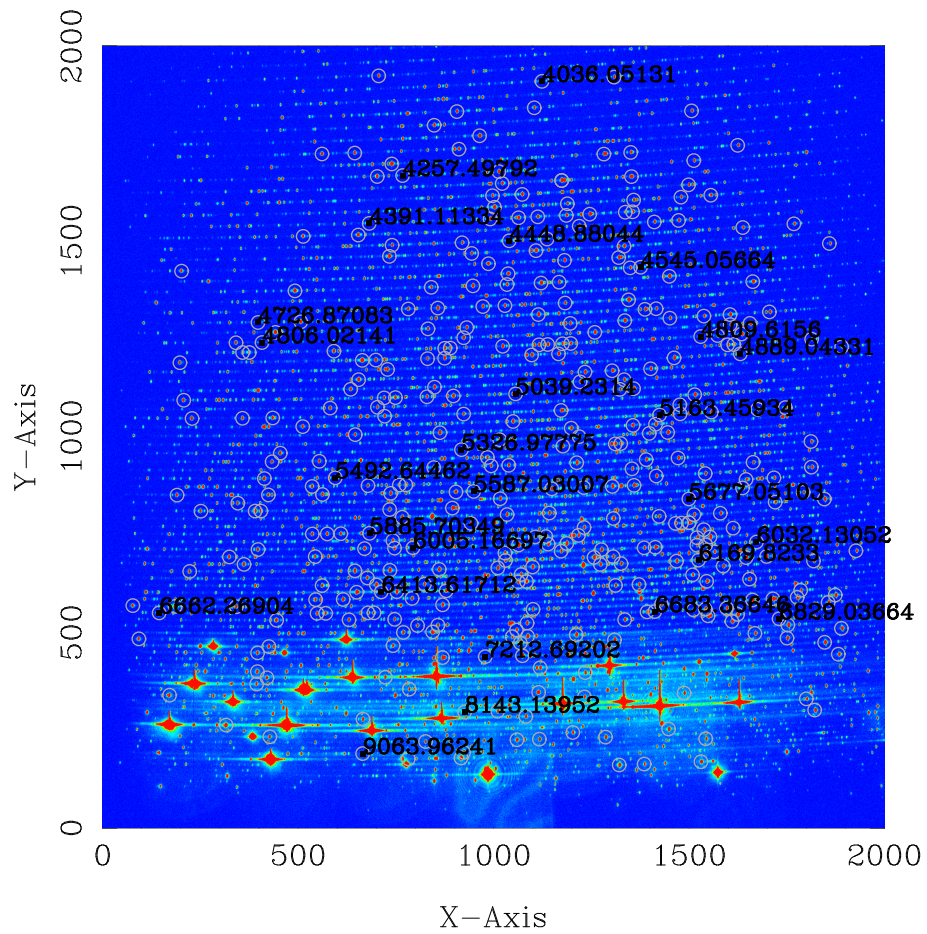
Figure 18: Raw frame of a ThAr lamp, used for wavelength calibration. The different emission lines identified by the pipeline are marked with circles. We label the wavelength of one of each 15 emission lines.
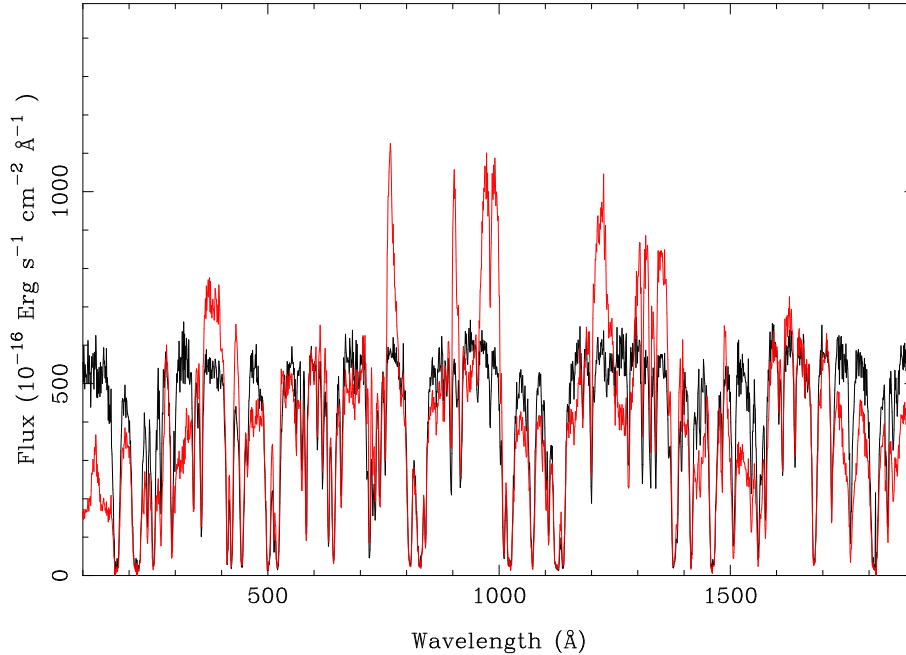
Figure 19: CAFE: Effect of the flat-field correction. The red line shows the spectrum corresponding to order 60 for a non flat-fielded frame, compared to the flat-fielded one (in white)

frames obtained along the commissioning run were combined and then reduced (up to the indicated reduction step). Then the reduced frames was normalized order by order to an average value of one.

To correct for the flat-fielding the reduced frames should be divided by this master flat-field frame. To cross-check the quality of this correction, it was applied to each of the continuum frames observed along the commissioning run. The corrected frames have a `rms` of 2% of the avearage flux. This is basically the accuracy of the flat-field correction.

- Once extracted both the science and arc frames, the wavelength calibration is done order by order by a two-step iterative procedure. First, a set of well identified emission lines (matched manually order-by-order) is matched again with the corresponding emission lines and a low-order polynomial function solution is found to the wavelength calibration. Figure 18 shows an example of a ThAr ARC lamp with the initially identified emission lines highlightled with circles. The wavelength of one of each 15th has been labelled to illustrate the line identification.

  Once a preliminar wavelength solution is found, the pipeline looks for a large database of ThAr emission lines (extracted from the NIST database), that matches with the wavelength corresponding to each considered order, and re-identify the detected lines in the ARC with this catalogue. Then the pipeline determine the new wavelength solution, using a higher order polynomial function (two orders lower than the number of identified lines), ranging between 4 and 14, in general.

  An example of these procedure is illustrated in Figure 20. The complete list of ARC-lines can be found in following webpage `http://www.caha.es/sanchez/cafe/orders.html`.

- Flux calibration. The flux calibration was performed based on the master counts-to-flux transformation created to derive the efficiency of the instrument. These counts-to-flux transformation was derived by reducing all the calibration stars frames observed along the night of the 17th of July, comparing them with the published flux-calibrated spectra (Oke 1990), and deriving the transformation between counts/seconds to flux-units. The flux calibrated frames are in units of 10^{-16} Erg$\cdot$s^{-1}A^{-1}cm^{-2}.

The final dataproduct of the pipeline is a two RSS frame, with the spectrum corresponding to each order stacked in consecutive rows. The wavelength solution has been included in the header using two different set of keywords:

- The standard IRAF header keyword for Echelle spectroscopy, based on the `WAT0_001, WAT1_001`, and `WATN_0KK` keywords.
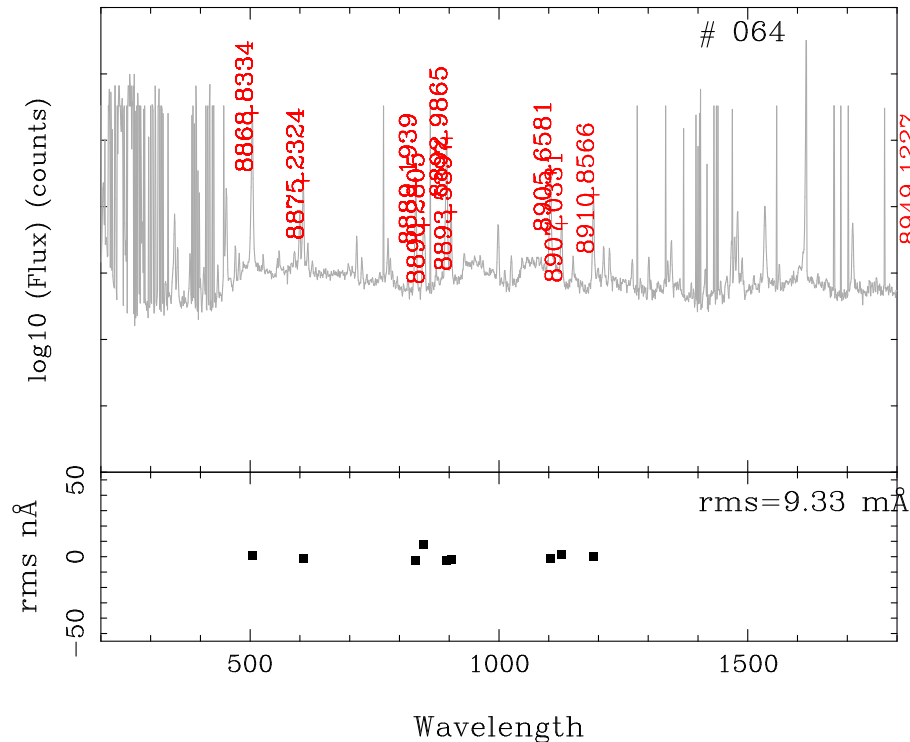
Figure 20: Example of the wavelength calibration solution and accuracy, corresponding to the order #124. The top panel shows the ThAr ARC-lamp spectrum corresponding to this order, including the wavelength of the identified emission lines. The bottom panel shows the difference between the nominal and recovered wavelength for these emission lines after wavelength calibration.

- An Ad-hoc created set of header keywords:
  - `PIX1_`*KK* Reference pixel of the wavelength calibration of the *KK*-order (or *KK* row in the FITs frame).
  - `VAL1_`*KK* Wavelength in Å associated with the reference pixel, for the *KK*-order.
  - `DLT1_KK` Wavelength set per pixel in Å/pix for the *KK*-order.

NOTE: TBD, a full-range spectrum created after combining all the orders' spexctra in a single one.

The pipeline includes some routines to visualize the reduced spectra, to allow the user to evaluate the quality of the data. These routines are:

- `spec2D_CAFE_plot.pl` (or `spec2D_CAFE_plot_SN.pl`) This script allow us to visualize a single order spectrum from a reduced RSS frame. In the first case, it shows just the reduced spectrum, while in the second one it plots both the spectrum and its corresponding S/N spectrum. Figure 16 was created with this script.

- `spec2D_CAFE_plot_all.pl` This scripts allows to visualize or hardcopy a complete spectrum, overlapping the different orders with different colors.

NOTE: TBD: A fair comparison with other non-automatic reduction procedures.

7   Acknowledgements

8   References

[Sánchez(2006)] Sánchez S. F., 2006, AN, 327, 850

—oOo—